We are IntechOpen, the world's leading publisher of Open Access books Built by scientists, for scientists

4,800
Open access books available

122,000
International authors and editors

135M
Downloads

Our authors are among the

154
Countries delivered to

TOP 1%
most cited scientists

12.2%
Contributors from top 500 universities

CLARIVATE ANALYTICS BOOK CITATION INDEX INDEXED

WEB OF SCIENCE™

Selection of our books indexed in the Book Citation Index in Web of Science™ Core Collection (BKCI)

Interested in publishing with us?
Contact book.department@intechopen.com

Numbers displayed above are based on latest data collected.
For more information visit www.intechopen.com

20

Fractional-Order Models for the Input Impedance of the Respiratory System

Clara Ionescu[1], Robin De Keyser[1], Kristine Desager[2] and Eric Derom[3]
[1]*Ghent University, Department of Electrical energy, Systems and Automation, Technologiepark 913, Gent 9052, Belgium*
[2]*University Hospital Antwerp, Department of Pulmonary Medicine, Campus Drie Eiken, D.T.428, Universiteitsplein 1, 2610 Wilrijk, Belgium*
[3]*Ghent University Hospital, Department of Respiratory Medicine, De Pintelaan 185, Gent 9000, Belgium*

1. Introduction

Thanks to the technological advances, complex mathematical tools have been enabled for general use and applications in the field of biomedical engineering. Moving from fiddler's paradise of integer order models for biological systems, the modern scientist has vast possibilities to explore new horizons in the novel generalized order modeling concepts (Losa *et al*, 2005).

One of these novel concepts in modeling and identification is that of fractals, self-similarity in geometrical structures (Mandelbrot, 1983). Although originally applied in mathematics and chemistry, the signal processing community introduced the concept of fractional order modelling in several areas (Eke *et al.*, 2002; Losa *et al*, 2005; Jesus *et al*, 2008). A perfect example of fractal structure is that of the lungs (Mandelbrot, 1983; Weibel, 2005) and of the circulatory system (Gabrys *et al*, 2004). Regarding the lungs, there exist observations to support the claim that dependence exists between the viscoelasticity and the air-flow properties in the presence of airway mucus with disease. It is also agreed that fractional orders appear intrinsically in viscoelastic materials (i.e. soft lung tissue, soft arterial tissue, polymers) (Suki *et al.,* 1994; Adolfsson *et al.,* 2005; Craiem & Armentano, 2007). When characterization of the respiratory tree is envisaged, the mechanical properties are captured by measuring the input impedance, which gives insight upon airway and tissue resistance and compliance (Oostveen *et al*, 2003; Ionescu & De Keyser, 2008; Ionescu *et al*, 2009b).

This chapter will discuss the use of fractional order (FO) models for characterizing the input impedance of the human respiratory system in relation to its fractal structure. Given a brief summary of our previously gathered insight in the intrinsic properties of human respiratory tree, we introduce here several competitive models for characterizing the total input impedance. A comparison with the well-inherited fractional order model from the specialized literature and recently published hot-stone articles, will situate our results within the overall research on this challenging topic.

2. Materials and Methods

2.1 Subjects

The first group evaluated in this study consists of volunteers without a history of respiratory disease, whose lung function tests were performed in our laboratory and Table 1 presents their biometric parameters, whereas a detailed analysis on their respiratory impedance parameters can be found in (Ionescu *et al*., 2009a).

HEALTHY	male (n=15)	female (n=8)
Age (yrs)	23±0.7	23±1.3
Height (m)	1.76±0.062	1.68±0.032
Weight (kg)	73±5.1	63±2.8

Table 1. Biometric parameters of the healthy subjects; values are presented as mean±SD (SD: standard deviation).

A second group consists of patients under observation at the "Leon Danielo" Hospital in Cluj-Napoca, Romania, pulmonary division, diagnosed with COPD (Chronic Obstructive Pulmonary Disease). The latter group of patients consisted of former coal miners from the Petrosani area in Romania. Table 2 presents the corresponding biometric and spirometric parameters of the COPD group (Ionescu & De Keyser, 2009c).

COPD	male (n=21)
Age (yrs)	58±9
Height (m)	1.81±0.08
Weight (kg)	76±4.8
VC % pred	86±6.7
FEV_1 % pred	43±9

Table 2. Biometric and spirometric parameters of the COPD patients. Values are presented as mean±SD; % pred: predicted according to the asymptomatic males of the present study; VC: vital capacity; FEV_1: forced expiratory volume in one second.

2.2 Measurement Procedure

In this study, the Forced Oscillations Technique (FOT) non-invasive lung function test was applied (Oostveen *et al.*, 2003). Air-pressure variations P, with respect to the atmospheric pressure and corresponding air-flow Q during the FOT lung function test can be measured either at the mouth of the patient, either endotracheal, either at body surface (Northrop, 2002). If the impedance is measured at the mouth of the patient, then it is called *input impedance*. In the case when the measurements are done across the body surface, this is then called *transfer impedance*. Using electrical analogy, where the P corresponds to voltage and Q corresponds to current, the respiratory impedance Z_r can be defined as their spectral (frequency domain) ratio relationship (Daröczy & Hantos, 1982). The present study is restricted to measurements of input respiratory impedance, that is, P and Q are measured at the mouth of the patient with reference to the atmospheric pressure (Oostveen *et al*., 2003).

Typically, the resulting impedance is a frequency dependent complex representation of mechanical properties and defines a real part R_{rs} – called *resistance* – and an imaginary part X_{rs} – called *reactance*. The real part describes the dissipative mechanical properties, whereas the imaginary part is related to the energy storage capacity and determined by both elastic and inertive properties.

The subject is connected to the typical setup from figure 1 via a mouthpiece, suitably designed to avoid flow leakage at the mouth and dental resistance artefact. The oscillatory flow U(t) in most recent FOT devices is generated by a loudspeaker (LS) connected to a chamber (Birch *et al.*, 2001). The LS is driven by a power amplifier fed with the oscillating signal generated by a computer. The movement of the LS cone generates a pressure oscillation inside the chamber, which is applied to the patient's respiratory system by means of a tube connecting the LS chamber and the bacterial filter (bf). A side opening (BT) of the main tubing allows the patient to decrease dead space re-breathing. Ideally, this bias tube will exhibit high impedance at the excitation frequencies to avoid the loss of power from the LS pressure chamber. It is advisory that during the measurements, the patient should wear a nose clip and keep the cheeks firmly supported to reduce the artefact of upper airway shunt. Pressure and flow are measured at the mouthpiece, respectively by means of **i)** a pressure transducer (PT) and **ii)** a pneumotachograph (PN) plus a differential pressure transducer (PT). The FOT pressure signal should be kept within a range of a peak-to-peak size of 0.1-0.3 kPa, in order to ensure optimality, patient comfort and stay within a narrow range in order to assume linearity (Desager *et al.*, 1997). Averaged measurements from 3-5 technically acceptable tests should be taken into consideration for further signal processing. Typical recorded signals are depicted in figure 1-B.

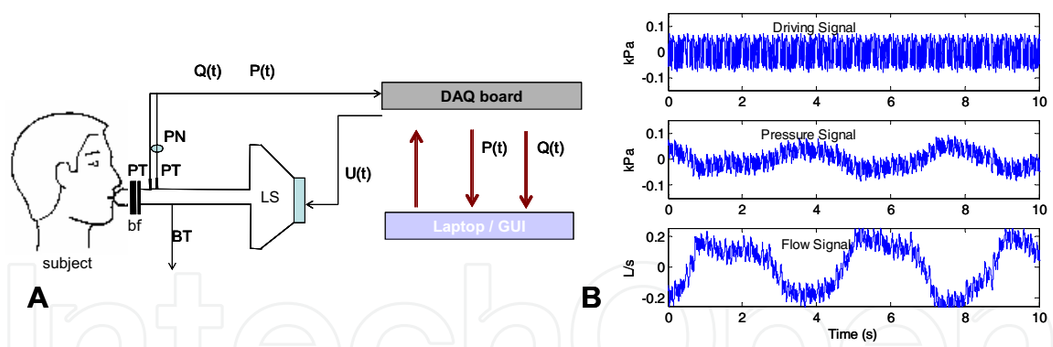

Fig. 1. (**A**) A schematic overview of the FOT measurement setup. (**B**) Typical measured signals from one subject: oscillatory driving pressure; trans-respiratory pressure and air-flow. The breathing of the patient (low frequency) can be observed superimposed on the multisine signals. See text for symbol explanations.

Several alternative setups for FOT have been developed during the last decades, such as the head plethysmograph (Govaerts *et al*, 1994), infants (Desager *et al*, 1991), or replacing the pneumotachograph by a known tube impedance (Franken *et al*, 1981).

The most common periodic excitation is the sinusoidal excitation; this signal is of great interest when frequency-domain identification is targeted, providing unbiased estimates. Besides, it allows direct interpretation of the mechanical load and poses a high signal-to-

noise ratio. The drawback is that only one point in the frequency domain is excited, so the information is not sufficient to assess the mechanical properties of the lungs. In order to avoid this drawback, *multi-sine waves* are applied to excite the system over the desired range of frequencies, in one experiment. The limitation, however, is that the amplitude (power) of the signal at a specific frequency decreases, due to the fact that the overall power spectrum of the multi-sine must be kept within the linearity, safety and comfort range for the patient. This constraint leads to limitations in the peak-to-peak amplitude of the FOT signal, i.e. between 0.1-0.3kPa (Oostveen *et al.*, 2003; Van De Woestijne *et al.*, 1994). In this study, we consider applying multi-sine oscillations in the frequency range: 4-48Hz. An overview of other type of signals is given in (Oostveen *et al.*, 2003; Ionescu *et al.*, 2009a).

3. Theoretical Background

The following sections provide the theoretical principles and experimental results underpinning the proposed fractional-order models.

3.1 Respiratory Input Impedance

One of the most common non-parametric representations of the *input impedance* Z_r is obtained assuming no correlation between the breathing and the excitation signal. This is done in the conditions that the breathing and the oscillations at the mouth of the patient are superimposed (Daröczi & Hantos, 1982), thus breathing can be considered as noise in this identification task. Apart from the errors introduced by the linear assumptions, the spectral representation of Z_r is a fast, simple and fairly reliable evaluation. The algorithm for estimating Z_r can be summarized starting from:

$$P(s) = Z_r(s)Q(s) + U_r(s) \tag{1}$$

where s denotes the Laplace operator. If the excitation signal is designed to be uncorrelated with the breathing of the patient and correlation analysis applied to the measured signals, one can estimate the respiratory impedance as:

$$\widehat{Z_r}(j\omega) = \frac{S_{PU_g}(j\omega)}{S_{QU_g}(j\omega)} \tag{2}$$

where $S_{ij}(j\omega)$ denotes the cross-correlation spectra between the various input-output signals, ω is the angular frequency and $j = (-1)^{1/2}$ and $U_g(t)$ denotes the excitation signal generated by the loudspeaker (multisine). From the point of view of the forced oscillatory experiment, the signal components of respiratory origin, (U_r) have to be regarded as pure noise for the identification task. However, to fulfill this condition it is necessary that:

i) the test signal U_g is designed such that it is not correlated with the normal respiratory breathing signal U_r and
ii) the conversion from voltage to pressure oscillation follows a linear relationship.

By definition, the modulus $|Z_r|$ is a measure of the total mechanical load of the respiratory system at the respective oscillation frequencies. The phase of respiratory impedance Φ_r is defined as the phase lag between $P(t)$ and $Q(t)$ and it is computed as the ratio between the time lag and the oscillation period T: $\Phi_r = 360 \times \Delta t / T$. The frequency where Φ_r =0 is called the *resonance frequency* and it depends on the balance between the different kind of mechanical properties (elastic, inertial). This then allows for differentiating between healthy and pathologic cases, since the resonance frequency changes significantly from typically 8Hz for a healthy adult to 14Hz for a patient with mild airway obstruction and from 20Hz onward in cases of severe obstruction.

According to (Pasker *et al.,* 1997), the real (*Rrs*) and imaginary (*Xrs*) parts of the impedance can be predicted from their biometric data as given below:

Female

Rrs0f=-0.4300*h+0.00165*w-0.00070*a+0.9312 (RSD=0.0619)
Rrs1f=0.01176*h-0.000106*w-0.000045*a-0.00817 (RSD=0.00256)
Xrs0f=0.2487*h-0.001700*w-0.00053*a-0.2158 (RSD=0.0406)

Male

Rrs0m=-0.2454*h+0.001564*w-0.00055*a+0.5919 (RSD=0.0493)
Rrs1m=0.01176*h-0.000106*w-0.000045*a-0.00817 (RSD=0.00197)
Xrs0m=0.2487*h-0.001700*w-0.00053*a-0.2158 (RSD=0.0306)

where *a* denotes age in *yrs*, *h* denotes height in *m*, *w* denotes weight in *kg* and *RSD* is the residual standard deviation. The *0f* and *1f* coefficients are related to the *E* and *D* coefficients respectively, resulting from fitting the polynomial given by:

$$R_{rs} \ (\text{or } X_{rs}) = Df + E \tag{3}$$

to the real or imaginary data sets, with *D, E* identified constants and *f* the oscillatory frequency, in this case between 4-48Hz. Confidence intervals of the identified values for 95% were calculated from RSDx1,96.

With the real (*Rrs*) and imaginary (*Xrs*) parts of the impedance from (2), parametric identification can be performed and the model parameters estimated using a nonlinear least squares optimization algorithm, by use of the MatLab® function *lsqnonlin*. The optimization algorithm is a subspace trust region method and is based on the interior-reflective Newton method described in (Coleman *et al*, 1996). In this application, the lower bounds were set to 0 (model parameters cannot have negative values) and no upper bounds. The optimization stopped either when a high number of iterations reached 100*nr. of variables, or a termination tolerance value of 1*e*-8. In all cases we obtained a correlation coefficient between data and model estimates above 80%.

Along with the corresponding model estimates, the error on the real and imaginary part respectively and the total error between the real patient impedance and the model estimated impedance are calculated according to the formulae:

$$E_R = \sqrt{\frac{1}{N}\sum_{1}^{N}(r-\hat{r})^2}; \quad E_X = \sqrt{\frac{1}{N}\sum_{1}^{N}(x-\hat{x})^2}; \qquad E_{Total} = \sqrt{E_R^2 + E_X^2} \tag{4}$$

with r denoting values in the real part of the impedance, x denoting values in the imaginary part of the impedance and N the total number of data samples (N=23).

3.2 Data Validation and Statistical Analysis

Since the healthy groups consisted of volunteers with no record of respiratory pathology, a validation was done using the reference values given in the previous section. All patients were within the 95% confidence intervals (Ionescu *et al*. 2009a). An one-way analysis of variance (*t* student test) was used to compare model parameters among the two groups: healthy and COPD. Results were considered significant at $p \le 0.05$. Further on, model parameters from the separate groups were evaluated using boxplots. The boxplot is typically a box and whisker plot for each column of the matrix, whereas here the columns are respectively the parameters for healthy group and for COPD group. The box has lines at the lower quartile, median, and upper quartile values. The whiskers are lines extending from each end of the box to show the extent of the rest of the data. Outliers are data with values beyond the ends of the whiskers (see, e.g. figure 5).

3.3 The Origins of Fractional-Order Models

The concept of fractional order (or non-integer order) systems refers to those dynamical systems whose parameters contain arbitrary order derivatives and/or integrals. The FO derivatives and integrals are tools of the Fractional Calculus theory (Podlubny, 1999). The dynamical systems whose model can be represented in a natural way by FO parameters, exhibit specific features:

- viscoelasticity;
- diffusion;
- fractal structure.

Viscoelasticity has been shown to be the origin of the appearance of FO models in polymers (from the Greek: *poly* - many and *meros* -- parts) (Adolfsson *et al*, 2005) and other resembling biological tissues (Suki *et al*, 1994). Diffusion phenomena have been intensively studied in the field of chemistry and dielectrics (Oustaloup, 1995; Machado & Jesus, 2004) and only recently in biology (Losa *et al*, 2005). Finally, it has been shown that the fractal structure leads to a FO model in some geometrical structures and electrical networks (Oustaloup, 1995; Ramus *et al*, 2002). Although viscoelastic and diffusive properties were intensively investigated in the respiratory system, the fractal structure was surprisingly ignored. Probably one of the reasons is that the respiratory system is not symmetric, thus failing to satisfy one of the conditions for being a typical fractal structure. Nonetheless, some degree of recurrence has been recognized in the airway generation models (Mandelbrot, 1983; Weibel, 2005), but simulation models including this specific property are not yet available.

The literature reports the existence of a FO model based on viscoelastic assumptions (Hantos *et al*, 1992). The model provides an expression for the input impedance (measured at the mouth of the patient) as:

$$Z_r(s) = \frac{P(s)}{Q(s)} = R + Ls + \frac{1}{Cs^{\beta}} \tag{5}$$

with P - pressure in kPa; Q - flow in l/s; Z_r - the impedance; R - airway resistance kPa-s/l; L - inductance kPa-s^2/l; C - capacitance in l/kPa; $0 \leq \beta \leq 1$ a fractional order and s the Laplace operator. This model, although broadly used by researchers and providing valid parameter values in several groups of patients, is unable to characterize increasing resistance with frequency at frequencies higher than 30Hz (Ionescu & De Keyser, 2008). As a result of the limitation, researchers have performed and reported studies in which the parameter values are meaningless from a physiological standpoint, i.e. negative (Hantos *et al*, 1982; Suki *et al*, 1997).

In the same context of characterizing viscoelasticity, (Suki *et al,* 1994) established possible scenarios for the origin of viscoelastic behaviour in the lung parenchyma. The authors apply the model from (5) in the form:

$$Z_r(s) = \frac{1}{Cs^{\beta}} \tag{6}$$

in which the real part denotes elastance and the imaginary part the viscance of the tissue. Similarly to (5), this model was also referred as the *constant-phase model* because the phase is independent with frequency, implying a frequency-independent mechanical efficiency (Oustaloup, 1995).

In his paper, Suki *et al.* (1994) recognizes five classes of systems admitting power-law relaxation or constant-phase impedance:

- **Class 1**: *systems with nonlinear constitutive equations*; a nonlinear differential equation may have a At^{-n} solution to a step input. Indeed, lung tissue behaves nonlinearly, but this is not the primary mechanism for having constant-phase behaviour, since the forced oscillations are applied with small amplitude to the mouth of the patient to ensure linearity.
- **Class 2**: *systems in which the coefficients of the constitutive differential equations are time-varying;* the linear dependence of the pressure-volume curves in logarithmic time scale does not support this assumption.
- **Class 3**: *systems in which there is a continuous distribution of time constants that are solutions to integral equations*. By aid of Kelvin bodies and an appropriate distribution function of their time constants, a linear model has been able to capture the hysteresis loop of the lungs, capturing the relaxation function decreasing linearly with the logarithm of time. This is a class of systems which may be successful in acknowledging the origin of the constant-phase behaviour, but there is no micro--structural basis.
- **Class 4**: *complex dynamic systems exhibiting self-similar properties (fractals)*. This class is based on the fact that the scale-invariant behaviour is ubiquitous in nature and the stress relaxation is the result of the rich dynamic interactions of tissue strips independent of their individual properties. Although interesting, this theory does not give a straightforward explanation for the appearance of constant-phase behaviour.

- **Class 5**: *systems with input-output relationships including fractional order equations*; borrowed from fractional calculus theory, several tools were used to describe viscoelasticity by means of fractional order differential equations (Suki *et al*, 1997; Craiem & Armentano, 2007).

Referring to the specific application of respiratory mechanics, Classes 3-5 are most likely to characterize the properties of lung parenchyma. The work presented in this chapter deals primarily with concepts from Class 4, but addresses also several items from Class 5.

Hitherto, the research community focused on the aspect of viscoelasticity in soft biological tissues. The other property of the lungs which can be related to fractional-order equations is diffusion and some papers discuss this aspect (Losa *et al*, 2005).

Surprisingly, the plain fractal-like geometry of the airways has been completely ignored throughout the decades. Perhaps one of the reasons for this lack of interest from the research community is that the lungs are not perfectly symmetric and even more, the quasi-symmetry disappears completely with disease. While most biologic processes could be described by models based on power law behaviour and quantified by a single characteristic parameter (one fractional order), the necessity arises to introduce multi-fractal models. The study presented in this chapter will address both the single- and multi-fractal models for the respiratory impedance.

3.4 Some Concepts from Fractional Calculus

The fractional calculus is a generalization of integration and derivation to non-integer (fractional) order operators: D_t^n. Several definitions of this operator are available; see e.g. (Podlubny, 1999). All of them generalize the standard differential--integral operator in two main groups:

(a) they become the standard differential--integral operator of any order when *n* is an integer;

(b) the Laplace transform of the operator D_t^n is s^n (provided zero initial conditions), and hence the frequency characteristic of this operator is $(j\omega)^n$.

The Laplace transform for integral and derivative order *n* are, respectively:

$$\begin{aligned} L\left\{D_t^{-n} f(t)\right\} &= s^{-n} F(s) \\ L\left\{D_t^{n} f(t)\right\} &= s^{n} F(s) \end{aligned} \tag{7}$$

where $F(s) = L\left\{f(t)\right\}$ and *s* is the Laplace variable. The Fourier transform can be obtained by replacing *s* with *jω* in the Laplace transform and the equivalent frequency-domain expressions are:

$$\begin{aligned} \frac{1}{(j\omega)^n} &= \frac{1}{\omega^n}\left(\cos\frac{\pi}{2} + j\sin\frac{\pi}{2}\right)^{-n} = \frac{1}{\omega^n}\left(\cos\frac{n\pi}{2} - j\sin\frac{n\pi}{2}\right) \\ (j\omega)^n &= \omega^n\left(\cos\frac{\pi}{2} + j\sin\frac{\pi}{2}\right)^{n} = \omega^n\left(\cos\frac{n\pi}{2} + j\sin\frac{n\pi}{2}\right) \end{aligned} \tag{8}$$

Thus, the modulus and the argument of the FO terms are given by:

$$\begin{aligned} \left|M\right|_{dB} &= 20\log\left|(j\omega)^{\mp n}\right| = \mp 20n\log\left|\omega\right| \\ \angle\left|_{rad}\right. &= \arg\left((j\omega)^{\mp n}\right) = \mp n\frac{\pi}{2} \end{aligned} \tag{9}$$

resulting in:

- a Nyquist contour of a beeline with a slope $\mp n\frac{\pi}{2}$ anticlockwise rotation of the real axis in the complex plane around the origin according to variation of the FO value n;
- Magnitude (dB *vs* log-frequency): straight line with a slope of $\mp 20n$ passing through 0dB for $\omega = 1$ (see figure 2);
- Phase (rad *vs* log-frequency): horizontal line, thus independent with frequency, with value $\mp n\frac{\pi}{2}$ (see figure 2).

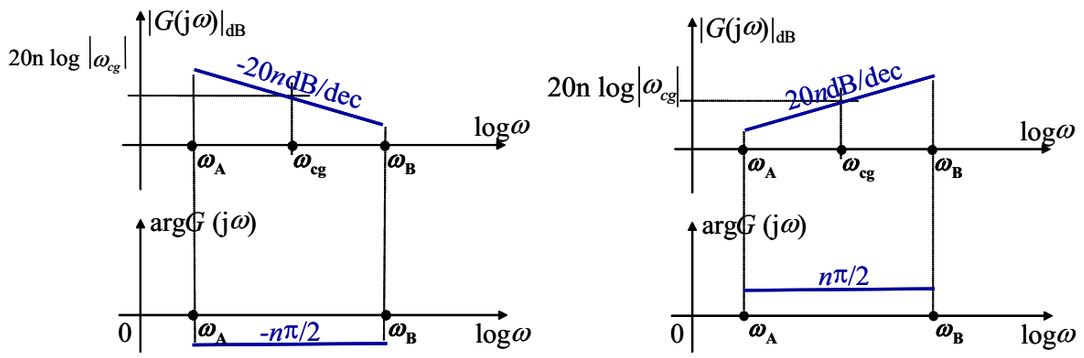

Fig. 2. Sketch representation of the FO integral and derivate operators in frequency domain, by means of the Bode plots (Magnitude, Phase)

4. Proposed Fractional-Order Models for Evaluation

Several attempts have been made to obtain an electrical equivalent of the respiratory tree (Farre *et al*, 1989; Diong *et al,* 2007). However, the models reported hitherto are an approximation of the tree rather than a precise formulation, and do not preserve the intrinsic geometry. Thanks to technological advances, information on airway radius, length and thickness is available. Our previous work provides a simulator for the dichotomous airway structure and validates the appearance of the fractional-order behaviour in the impedance, arising intrinsically from the fractal structure of the lungs (Ionescu *et al*, 2009d; Muntean *et al*, 2009).

The FO terms in the impedance models arise either from intrinsic viscoelastic (at low frequencies), either intrinsic fractal structure of the airway tree. Viscoelastic properties and FO models have been already presented and validated for the respiratory tree in (Suki *et al*, 1994; Hantos *et al*, 1992). Furthermore, based on electrical analogy to ladder networks and corresponding theoretical background (Oustaloup, 1995), we have shown that the FO properties expressed in (9) arise from the fractal structure of the airway tree (Ionescu *et al*, 2009d). A similar analysis was conducted for other systems, e.g. the arterial tree (Gabrys *et al*, 2004) and the stemming leaf-structure (Ionescu & Machado, *in pres*s).
It is interesting to compare the models existing in literature with some similar candidate models, on the same range of frequencies 4-48Hz, which is commonly evaluated in clinical trials (Oostveen *et al*., 2003). We therefore propose the following FO models, in order of complexity. The first model, from here-on referred to as FO1, is based on (5):

$$Z_{FO1}(s) = R_1 + \frac{1}{C_1 s^{\beta_1}} \tag{10}$$

with R_1 the resistance, C_1 the capacitance and $0 \leq \beta \leq 1$. This model was initially used at frequencies<5Hz, whereas the effect of the inductance is negligible. Therefore, evaluating such model at 4-48Hz frequency interval, one may expect low performance results.
The second model proposed here, referred to as FO2, is in fact (5), by adding the inductance term:

$$Z_{FO2}(s) = R_2 + L_2 s + \frac{1}{C_2 s^{\beta_2}} \tag{11}$$

As frequency increases, the real part of the impedance may increase its value in some patients. The real part of (11) depends on the resistance R_2 and the capacitance term C_2 (the latter being frequency-dependent). As frequency increases, the real part of the term in C_2 decreases, therefore unable to characterize correctly the impedance. However, if the model is evaluated in a frequency range in which the real part of the impedance is decreasing with frequency, the model has good performance.
The third model (FO3) proposed for evaluation is based on (11), but the FO term is in the inductance and not in the capacitance:

$$Z_{FO3}(s) = R_3 + L_3 s^{\alpha_3} + \frac{1}{C_3 s} \tag{12}$$

This model will provide good results for patients with increasing impedance values with frequency in the real part, since the term in L_3 is directly proportional to frequency.
The last model proposed for evaluation in this chapter is based on our previous work (Ionescu *et al*., 2009a; Ionescu & De Keyser, 2009b), i.e. the multi-fractal model:

$$Z_{FO4}(s) = L_4 s^{\alpha_4} + \frac{1}{C_4 s^{\beta_4}} \tag{13}$$

which does not contain the resistance term R_4. The decision to eliminate this term was taken as a result of previous investigation, showing that the identified values are negligible (Ionescu & De Keyser, 2009b). Physically, the term in R_4 is not necessary, since the theory of fractional order appearance in ladder networks shows that the effects of R_4 are indirectly captured in the values of the FO terms and FO coefficients (Oustaloup, 1995; Ionescu *et al.*, 2009d).

5. Results

The complex impedance values for the healthy and COPD patients have been obtained using (2) and they are depicted in figure 3 below. It can be observed that the healthy group has a resonant frequency (zero crossing in the imaginary part) around 8 Hz, whereas the COPD group around 16 Hz. This shows that the lung parenchyma in COPD patients is less elastic than in healthy subjects. The real part denotes mainly the mechanical resistance of the lung tissue, which is generally increased in the COPD group, resulting in higher work of breathing. Also, the resistance at low frequencies is much increased in the COPD group, suggesting increased damping of the lung parenchyma (viscoelasticity is mainly analyzed at low frequencies). In both cases, the real part of the impedance decreases with frequency until 10-15Hz, and the low frequency interval becomes more significant with pathology.

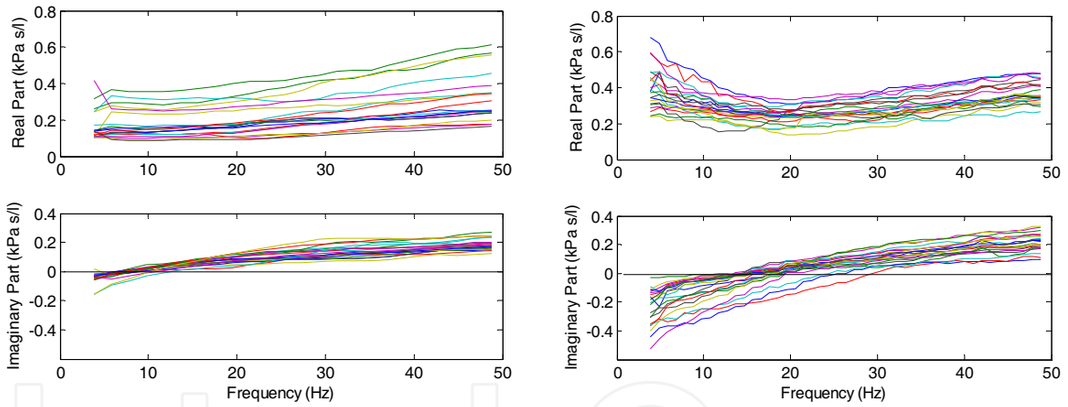

Fig. 3. Impedance plots for the healthy (left) and for the COPD (right) groups.

Next, the models from (10)-(13) are fitted to the complex impedance values. The results for model identification are obtained using the System Identification Toolbox within the MatLab platform, i.e. the *lsqnonlin* optimization function. The estimated parameter values along with the real, imaginary and total error values are given in Table 3 for the healthy subjects, respectively in Table 4 for the COPD patients.

Healthy	FO1	FO2	FO3	FO4
R	0.22±0.09	0.22±0.09	0.06±0.06	-
L	-	0.0007±0.0001	0.029±0.0302	0.0374±0.031
α	-	-	0.48±0.13	0.43±0.1
1/C	0	1.36±0.98	3.52±1.67	2.02±1.47
β	0.99±0.0006	0.99±0.01	-	0.79±0.16
$\mathbf{E_R}$	0.05±0.02	0.05±0.02	0.02±0.01	0.02±0.01
$\mathbf{E_X}$	0.12±0.02	0.01±0.006	0.015±0.0063	0.013±0.006
$\mathbf{E_T}$	0.13±0.03	0.05±0.02	0.02±0.01	0.02±0.01

Table 3. Estimated model parameters and modelling errors for the healthy group

COPD	FO1	FO2	FO3	FO4
R	0.18±0.08	0.26±0.08	0.27±0.05	-
L	-	0.0009±0.0001	0.0021±0.0014	0.015±0.008
α	-	-	0.87±0.1	0.59±0.09
1/C	1.73±3.32	5.20±2.49	8.9±3.79	2.94±1.54
β	0.18±0.36	0.83±0.16	-	0.52±0.11
$\mathbf{E_R}$	0.05±0.01	0.04±0.01	0.04±0.01	0.03±0.01
$\mathbf{E_X}$	0.14±0.02	0.02±0.006	0.03±0.011	0.02±0.006
$\mathbf{E_T}$	0.15±0.02	0.05±0.01	0.05±0.02	0.04±0.01

Table 4. Estimated model parameters and modelling errors for the COPD group

From the model parameters, one can calculate the tissue damping $G = \frac{1}{C}\cos\left(\frac{\pi}{2}\beta\right)$ and tissue elastance $H = \frac{1}{C}\sin\left(\frac{\pi}{2}\beta\right)$ (Hantos *et al*, 1992) and tissue histeresivity $\eta = G/H$ (Fredberg and Stamenovic, 1989). The relationship with (5) is found if the terms in C are re-written as:

$$\frac{1}{C\omega^{\beta}}\cos\left(\frac{\pi}{2}\beta\right) - j\frac{1}{C\omega^{\beta}}\sin\left(\frac{\pi}{2}\beta\right) = \frac{G - jH}{\omega^{\beta}} \tag{14}$$

From Tables 3 and 4 one may observe that the model FO4 gives the smallest total error. This is due to the fact that two FO terms are present in the model structure, allowing both a decrease and increase in values of the impedance with frequency. The FO2 model is the most commonly employed in clinical studies, with similar errors for the imaginary part, but higher error in the real part of the impedance than the FO4 model. The underlying reason is that the model can only capture a decrease in real part values of the impedance with frequency, whereas some patients may present an increase. As an example, figure 4 presents such a case, where one can visually compare the performance of the FO2 and FO4 models.

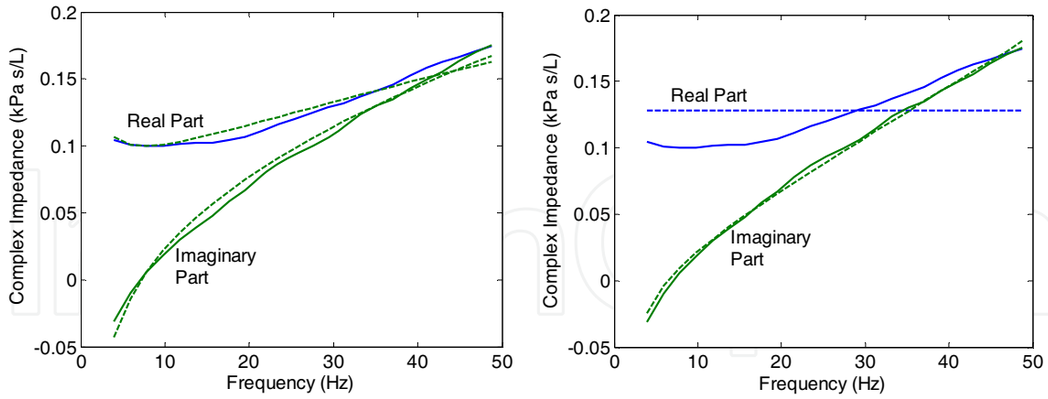

Fig. 4. A healthy subject data evaluated with FO4 (left) and with FO2 (right); continuous lines denote the measured impedance and dashed lines denote the identified impedance.

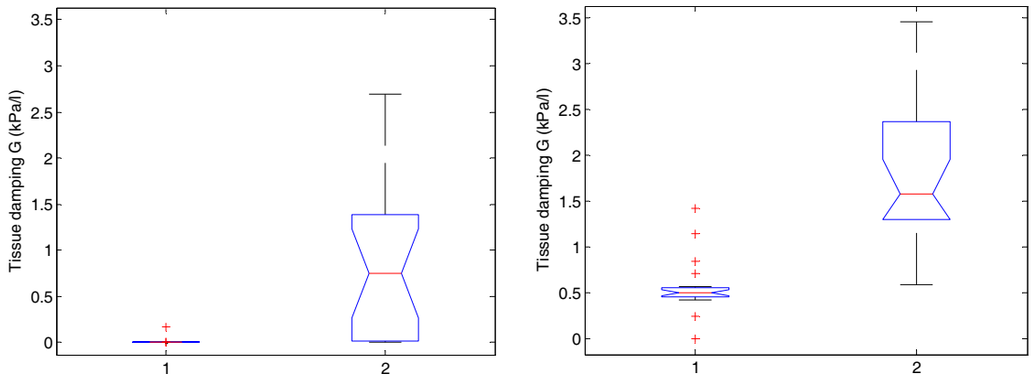

Fig. 5. Tissue damping G (kPa/l) with FO2, $p<3e^{-5}$ (left) and with FO4, $p<1e^{-8}$ (right); 1: Healthy subjects and 2: COPD patients.

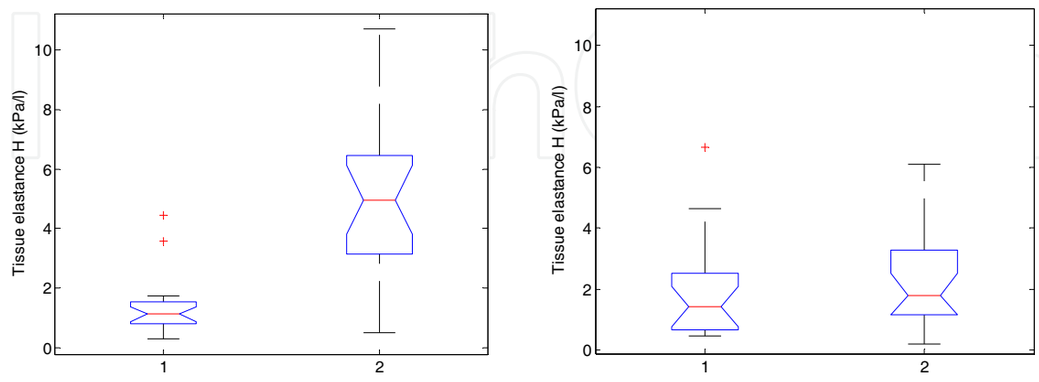

Fig. 6. Tissue elastance H (kPa/l) with FO2, $p<0.0012$ (left) and with FO4, $p<0.0004$ (right); 1: Healthy subjects and 2: COPD patients.

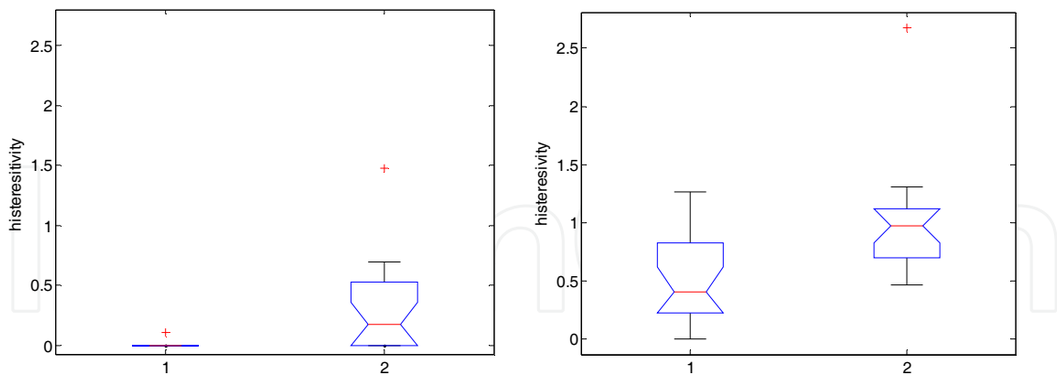

Fig. 7. Tissue hysteresivity η with FO2, p<0.0012 (left) and with FO4, p<0.0004 (right); 1: Healthy subjects and 2: COPD patients.

Figures 5, 6 and 7 depict the boxplots for the FO2 and FO4 for the tissue damping G, tissue elastance H and histeresivity η. Due to the fact that FO2 has higher errors in fitting the impedance values, the results are no further discussed. Although a similarity exists between the values given by the two models, the discussion will be focused on the results obtained using FO4.

Because FO are natural solutions in dielectric materials, it is interesting to look at the permittivity property of respiratory tissues. In electric engineering, it is common to relate permittivity to a material's ability to transmit (or *permit*) an electric field. By electrical analogy, changes in trans-respiratory pressure relate to voltage difference, and changes in air-flow relate to electrical current flows. When analyzing the permittivity index, one may refer to an increased permittivity when the same amount of air-displacement is achieved with smaller pressure difference. In other words, the hysteresivity coefficient incorporates this property for the capacitor, that is, the COPD group has an increased capacitance, justified by the pathology of the disease. Many alveolar walls are lost by emphysematous lung destruction, the lungs become so loose and floppy that a small change in pressure is enough to maintain a large volume, thus the lungs in COPD are highly compliant (elastic) (Barnes, 2000; Hogg, 2004; Derom *et al.*, 2007). The complex permittivity has a real part, related to the stored energy within the medium and an imaginary part related to the dissipation (or loss) of energy within the medium. The imaginary part of permittivity corresponds to:

$$\varepsilon = L \sin\left(\frac{\pi}{2}\alpha\right) \tag{15}$$

If the values are positive, (15) denotes the absorption loss. In COPD, due to the sparseness of the lung tissue, the air-flow in the alveoli is low, thus a low level of energy absorption is observed in figure 8. In healthy subjects, due to increased alveolar surface, higher levels of energy absorption are present, thus increased permittivity.

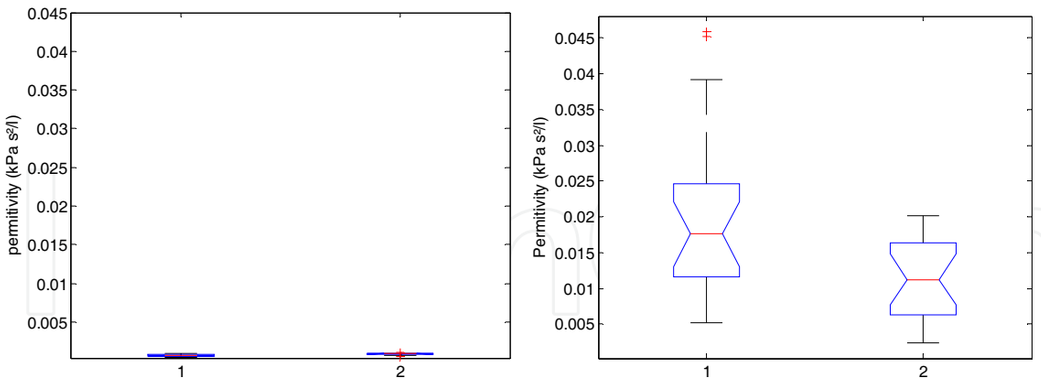

Fig. 8. Boxplots for the computed permittivity index ε in the FO2, p<0.0081 (left) and in FO4, p<0.0002 (right), in the two groups; 1: Healthy subjects and 2: COPD patients.

Another significant observation is that in general, FO4 identified more statistically significant model parameter values than FO2. In figures 5-7 FO4 parameters had identified similar variations between healthy and COPD groups. However, in figure 8, one can observe that FO4 identified a more realistic variation between healthy and COPD groups, i.e. a decreased permitivity index in COPD than in healthy.

6. Discussion

Tissue destruction (emphysema, COPD) and changes in air-space size and tissue elasticity are matched with changes in model parameters when compared to the healthy group. The physiological effects of chronic emphysema are extremely varied, depending on the severity of the disease and on the relative degree of bronchiolar obstruction versus lung parenchymal destruction (Barnes, 2000). Firstly, the bronchiolar obstruction greatly increases airway resistance and results in increased work of breathing. It is especially difficult for the person to move air through the bronchioles during expiration because the compressive force on the outside of the lung not only compresses the alveoli but also compresses the bronchioles, which further increase their resistance to expiration. This might explain the decreased values for inertance (air mass acceleration), captured by the values of L in the FO4. Secondly, the marked loss of lung parenchyma greatly decreases the elastin cross-links, resulting in loss of attachments (Hogg, 2004). The latter can be directly related to the fractional-order of compliance, which generally expresses the capability of a medium to propagate mechanical properties (Suki *et al.*, 1994).

The damping factor is a material parameter reflecting the capacity for energy absorption. In materials similar to polymers, as lung tissue properties are very much alike polymers, damping is mostly caused by viscoelasticity, i.e. the strain response lagging behind the applied stresses (Suki *et al.*, 1994;1997). In both FO models, the exponent β governs the degree of the frequency dependence of tissue resistance and tissue elastance. The increased lung elastance $1/C$ (stiffness) in COPD results in higher values of tissue damping and tissue elastance, as observed in Figures 5 and 6. The loss of lung parenchyma (empty spaced lung), consisting of collagen and elastin, both of which are responsible for characterizing lung elasticity, is the leading cause of increased elastance in COPD. The hysteresivity coefficient η

introduced in (Fredberg & Stamenovic, 1989) is G/H in this model representation. Given the results observed in Figure 7, it is possible to distinguish between tissue changes from healthy to COPD case. Since pathology of COPD involves significant variations between inspiratory and expiratory air-flow, an increase in the hysteresivity coefficient η reflects increased inhomogeneities and structural changes in the lungs.

It is difficult to provide a fair comparison between the values reported in this study and the ones reported previously for tissue damping and elastance. Firstly, such studies have been previously performed from excised lung measurements and invasive procedures (Suki *et al*. 1997; Brewer *et al.,* 2003; Ito *et al*., 2007), which related these coefficients with *transfer impedance* instead of *input impedance*. The measurement location is therefore important to determine mechanical properties of lungs. The data reported in our study, has been derived from non-invasive measurements at the mouth of the patients, therefore including upper airway properties. Secondly, the previously reported studies were made either on animal data (Hantos *et al*., 1992a;1992b; Brewer *et al*., 2003; Ito *et al*., 2007), either on other lung pathologies (Kaczka *et al.,* 1999).

Another interesting aspect to note is that in the normal lung, the airways and lung parenchyma are interdependent, with airway caliber monotonically increasing with lung volume. In emphysematous lung, the caliber of small airways changes less than in the normal lung (defining compliant properties) and peripheral airway resistance may increase with increasing lung volume. At this point, the notion of space competition has been introduced (Hogg, 2004), hypothesizing that enlarged emphysematous air spaces would compress the adjacent small airways, according to a nonlinear behavior. Therefore, the compression would be significantly higher at higher volumes rather than at low volumes, resulting in blunting or even reversing the airway caliber changes during lung inflation. This mechanism would therefore explain the significantly marked changes in model parameters in tissue hysteresivity depicted in figure 7. It would be interesting to notice that since small airway walls are collapsing, resulting in limited peripheral flow, it also leads to a reduction of airway depths. A correlation between such airway depths reduction in the diseased lung and model's non-integer orders might give insight on the progress of the disease in the lung.

The main limitation of the present study is that both model structures and their corresponding parameter values are valid strictly within the specified frequency interval 4-48Hz. Nonetheless, since only one resonant frequency is measured and is the closest to the nominal breathing frequencies of the respiratory system, we do not seek to develop model structures valid over larger frequency range. Moreover, it has been previously shown that one model cannot capture the respiratory impedance over frequency intervals which include more than one resonant frequency (Farré *et al*., 1989). A second limitation arises from the parameters of the constant-phase models. The fractional-order operators are difficult to handle numerically. The concept of modeling using non-integer order Laplace (e.g. $s^{\alpha}, \frac{1}{s^{\beta}}$) is rather new in practical applications and has not reached the maturity of integer-order system modeling. This concept has been borrowed from mathematics and chemistry applications to model biological signals and systems only very recently. Advances in technology and computation have enabled this topic in the latter decennia and it has captured the interest of researchers. Although the parameters are intuitively related to

pathophysiology of respiratory mechanics, the structural interpretation of the fractional-orders is in its early age.

Viscoelastic properties in lung parenchyma has been assessed in both animal and human tissue strips (Suki *et al*., 1994) and correlated to fractional-order terms. A relation between these fractional-orders and structural changes in airways and lung tissue has not been found (e.g. airway remodeling). In this line of thought, the mechanical properties of resistance, inertance and compliance have been derived from airway geometry and morphology (i.e. airway radius, thickness, cartilage percent, length, etc) (Ionescu *et al*., 2009b). These parameters have been employed in a recurrent structure of healthy lungs using analogue representation of ladder networks (Ionescu *et al*., 2009d). In the latter contribution, the appearance of a phase-lock (phase-constancy) is shown, supporting the argument that it represents an intrinsic property (Oustaloup, 1995). Its correlation to changes in airway morphology is an ongoing research matter. Experimental studies on various groups of patients (*e.g.* asthma *versus* COPD) to investigate a possible classification strategy for the parameters of this proposed model between various degrees of airway obstruction and lung abnormalities may also offer interesting information upon the sensitivity of model parameters.

7. Conclusions

This chapter presents a short overview on the properties of lung parenchyma in relation to fractional order models for respiratory input impedance. Based on available model structures from literature and our recent investigations, four fractional order models are compared on two sets of impedance data: healthy and COPD (Chronic Obstructive Pulmonary Disease). The results show that the two models broadly used in the clinical studies and reported in the specialized literature are suitable for frequencies lower than 15Hz. However, when a higher range of frequencies is envisaged, two fractional orders in the model structure are necessary, in order to capture the frequency dependence of the real part in the complex respiratory impedance. Since the real part may both decrease and increase within the evaluated frequency interval, there is need for both fractional order derivative and fractional order integral parameters.
The multi-fractal model proposed in this chapter provides statistically significant values between the healthy and COPD groups. Further investigations are planned in order to evaluate if the model is able to discriminate between various pathologies (e.g. asthma, cystic fibrosis and COPD).

Acknowledgements
C. Ionescu gratefully acknowledges the students who volunteered to perform lung function testing in our laboratory, and the technical assistance provided at University of Pharmacology and Medicine -"Leon Daniello" Cluj, Romania. This work was financially supported by the UGent-BOF grant nr. B/07380/02.

8. References

Adolfsson K., Enelund M., Olsson P., (2005), On the fractional order model of viscoelasticity, *Mechanics of Time-dependent materials,* Springer, 9, 15–34

Barnes P.J., (2000), Chronic Obstructive Pulmonary Disease, *NEJM Medical Progress*, 343(4), pp. 269-280

Birch M, MacLeod D, Levine M, (2001) An analogue instrument for the measurement of respiratory impedance using the forced oscillation technique, *Phys Meas*, 22, pp. 323-339

Brewer K., Sakai H., Alencar A., Majumdar A., Arold S., Lutchen K., Ingenito E., Suki B., (2003), Lung and alveolar wall elastic and hysteretic behaviour in rats: effects of in vivo elastase, *J. Applied Physiology*, 95(5), pp. 1926-1936

Craiem D., Armentano R., (2007) A fractional derivative model to describe arterial viscoelasticity, *Biorheology*, 44, pp. 251—263

Coleman, T.F. and Y. Li, (1996), An interior trust region approach for nonlinear minimization subject to bounds, *SIAM Journal on Optimization*, **6**, 418-445

Daröczy B, Hantos Z, (1982) An improved forced oscillatory estimation of respiratory impedance, *Int J Bio-Medical Computing*, **13**, pp. 221-235

Derom E., Strandgarden K., Schelfhout V, Borgstrom L, Pauwels R. (2007), Lung deposition and efficacy of inhaled formoterol in patients with moderate to severe COPD, *Respiratory Medicine*, 101, pp. 1931-1941

Desager K, Buhr W, Willemen M, (1991), Measurement of total respiratory impedance in infants by the forced oscillation technique*, J Applied Physiology*, 71, pp. 770-776

Desager D, Cauberghs M, Van De Woestijne K, (1997) Two point calibration procedure of the forced oscillation technique, *Med. Biol. Eng. Comput.,* 35, pp. 561-569

Diong B, Nazeran H., Nava P., Goldman M., (2007), Modelling human respiratory impedance, *IEEE Engineering in Medicine and Biology*, 26(1), pp. 48-55

Eke, A., Herman, P., Kocsis, L., Kozak, L., (2002) Fractal characterization of complexity in temporal physiological signals, *Physiol Meas,* 23, pp. R1-R38

Farré R, Peslin R, Oostveen E, Suki B, Duvivier C, Navajas D, (1989) Human respiratory impedance from 8 to 256 Hz corrected for upper airway shunt, *J Applied Physiology*, 67, pp. 1973-1981

Franken H., Clement J, Caubergs M, Van de Woestijne K, (1981) Oscillating flow of a viscous compressible fluid through a rigid tube, *IEEE Trans Biomed Eng*, 28, pp. 416-420

Fredberg J, Stamenovic D., (1989), On the imperfect elasticity of lung tissue, *J. Applied Physio*logy, 67:2408-2419

Gabrys, E., Rybaczuk, M., Kedzia, A., (2004) Fractal models of circulatory system. Symmetrical and asymmetrical approach comparison, *Chaos,Solitons and Fractals*, 24(3), pp. 707-715

Govaerts E, Cauberghs M, Demedts M, Van de Woestijne K, (1994) Head generator versus conventional technique in respiratory input impedance measuremenets, *Eur Resp Rev*, 4, pp. 143-149

Hantos Z., Daroczy B., Klebniczki J., Dombos K, Nagy S., (1982) Parameter estimation of transpulmonary mechanics by a nonlinear inertive model, *J Appl Physiol*, 52, pp 955--963

Hantos Z, Adamicza A, Govaerts E, Daroczy B., (1992) Mechanical Impedances of Lungs and Chest Wall in the Cat, *J. Applied Physiology*, 73(2), pp. 427-433

Hogg J. C., (2004), Pathophysiology of airflow limitation in chronic obstructive pulmonary disease, *Lancet*, **364**, pp. 709-21

Ionescu, C. & De Keyser, R. (2008). Parametric models for characterizing the respiratory input impedance. *Journal of Medical Engineering & Technology*, Taylor & Francis, 32(4), pp 315-324

Ionescu C., Desager K., De Keyser R., (2009a) Estimating respiratory mechanics with constant-phase models in healthy lungs from forced oscillations measurements, *Studia Universitatis Vasile Goldis Life Sciences Series, 19(1), pp. 123-132*

Ionescu C., Segers P., De Keyser R., (2009b) Mechanical properties of the respiratory system derived from morphologic insight, *IEEE Transactions on Biomedical Engineering*, April, 56(4), pp. 949-959

Ionescu C., De Keyser R., (2009c) Relations between Fractional Order Model Parameters and Lung Pathology in Chronic Obstructive Pulmonary Disease, *IEEE Transactions on Biomedical Engineering*, April, 56(4), pp. 978-987

Ionescu C., Oustaloup A., Levron F., De Keyser R., (2009d) "A model of the lungs based on fractal geometrical and structural properties", accepted contribution at the *15th IFAC Symposium on System Identification*, St. Malo, France, 6-9 July 2009

Ionescu C, Tenreiro-Machado J., (in press), Mechanical properties and impedance model for the branching network of the seiva system in the leaf of Hydrangea macrophylla, accepted for publication in *Nonlinear Dynamics*

Ito S., Lutchen K., Suki B., (2007), "Effects of heterogeneities on the partitioning of airway and tissue properties in mice", *J. Applied Physiology,* 102(3), pp. 859-869

Kaczka D., Ingenito E., Israel E., Lutchen K., (1999), "Airway and lung tissue mechanics in asthma: effects of albuterol", *Am J Respir Crit Care Med*, 159, pp. 169-178

Jesus I, Tenreiro-Machado J, Cuhna B., (2008), Fractional electrical impedances in botanical elements, Journal of Vibration and Control, 14, pp. 1389—1402

Losa G., Merlini D., Nonnenmacher T., Weibel E, (2005), *Fractals in Biology and Medicine*, vol.IV, Birkhauser Verlag, Basel.

Mandelbrot B. (1983) *The fractal geometry of nature*, NY: Freeman &Co

Machado, Tenreiro J., Jesus I., (2004), Suggestion from the Past?, *Fractional Calculus and Applied Analysis*, 7(4), pp. 403—407

Muntean I., Ionescu C., Nascu I., (2009) A simulator for the respiratory tree in healthy subjects derived from continued fraction expansions*, AIP Conference Proceedings vol. 1117: BICS 2008: Proceedings of the 1st International Conference on Bio-Inspired Computational Methods Used for Difficult Problems Solving: Development of Intelligent and Complex Systems, (*Eds): B. Iantovics, Enachescu C., F. Filip, ISBN: 978-0-7354-0654-4, *pp. 225-231*

Northrop R., (2002) *Non-invasive measurements and devices for diagnosis*, CRC Press

Oostveen, E., Macleod, D., Lorino, H., Farré, R., Hantos, Z., Desager, K., Marchal, F, (2003). The forced oscillation technique in clinical practice: methodology, recommendations and future developments, *Eur Respir J*, 22, pp 1026-1041

Oustaloup A. (1995) *La derivation non-entière* (in French), Hermes, Paris

Pasker H, Peeters M, Genet P, Nemery N, Van De Woestijne K., (1997) Short-term Ventilatory Effects in Workers Exposed to Fumes Containing Zinc Oxide: Comparison of Forced Oscillation Technique with Spirometry, *Eur. Respir. J.*, 10: pp. 523-1529

Podlubny, I. (1999). Fractional Differential Equations--*Mathematics in Sciences and Engineering*, vol. 198, Academic Press, ISBN 0125588402, New York.

Ramus-Serment M., Moreau X., Nouillant M, Oustaloup A., Levron F. (2002), Generalised approach on fractional response of fractal networks, *Chaos, Solitons and Fractals*, 14, pp. 479—488.

Suki, B., Barabasi, A.L., & Lutchen, K. (1994). Lung tissue viscoelasticity: a mathematical framework and its molecular basis. *J Applied Physiology,* 76, pp. 2749-2759

Suki B., Yuan H., Zhang Q., Lutchen K., (1997) Partitioning of lung tissue response and inhomogeneous airway constriction at the airway opening, *J Applied Physiology*, 82, pp. 1349--1359

Van De Woestijne K, Desager K, Duiverman E, Marshall F, (1994) Recommendations for measurement of respiratory input impedance by means of forced oscillation technique, *Eur Resp Rev*, 4, pp. 235-237

Weibel, E.R. (2005). Mandelbrot's fractals and the geometry of life: a tribute to Benoît Mandelbrot on his 80th birthday, in *Fractals in Biology and Medicine*, vol IV, Eds: Losa G., Merlini D., Nonnenmacher T., Weibel E.R., ISBN 9-783-76437-1722, Berlin: Birkhaüser, pp 3-16

Recent Advances in Biomedical Engineering

Edited by Ganesh R Naik

ISBN 978-953-307-004-9
Hard cover, 660 pages
Publisher InTech
Published online 01, October, 2009
Published in print edition October, 2009

The field of biomedical engineering has expanded markedly in the past ten years. This growth is supported by advances in biological science, which have created new opportunities for development of tools for diagnosis and therapy for human disease. The discipline focuses both on development of new biomaterials, analytical methodologies and on the application of concepts drawn from engineering, computing, mathematics, chemical and physical sciences to advance biomedical knowledge while improving the effectiveness and delivery of clinical medicine. Biomedical engineering now encompasses a range of fields of specialization including bioinstrumentation, bioimaging, biomechanics, biomaterials, and biomolecular engineering. Biomedical engineering covers recent advances in the growing field of biomedical technology, instrumentation, and administration. Contributions focus on theoretical and practical problems associated with the development of medical technology; the introduction of new engineering methods into public health; hospitals and patient care; the improvement of diagnosis and therapy; and biomedical information storage and retrieval. The book is directed at engineering students in their final year of undergraduate studies or in their graduate studies. Most undergraduate students majoring in biomedical engineering are faced with a decision, early in their program of study, regarding the field in which they would like to specialize. Each chosen specialty has a specific set of course requirements and is supplemented by wise selection of elective and supporting coursework. Also, many young students of biomedical engineering use independent research projects as a source of inspiration and preparation but have difficulty identifying research areas that are right for them. Therefore, a second goal of this book is to link knowledge of basic science and engineering to fields of specialization and current research. The editor would like to thank the authors, who have committed so much effort to the publication of this work.

How to reference

In order to correctly reference this scholarly work, feel free to copy and paste the following:

Clara Ionescu, Robin De Keyser, Kristine Desager and Eric Derom (2009). Fractional-Order Models for the Input Impedance of the Respiratory System, Recent Advances in Biomedical Engineering, Ganesh R Naik (Ed.), ISBN: 978-953-307-004-9, InTech, Available from: http://www.intechopen.com/books/recent-advances-in-biomedical-engineering/fractional-order-models-for-the-input-impedance-of-the-respiratory-system

INTECH
open science | open minds

InTech Europe
University Campus STeP Ri
Slavka Krautzeka 83/A

InTech China
Unit 405, Office Block, Hotel Equatorial Shanghai
No.65, Yan An Road (West), Shanghai, 200040, China

www.intechopen.com

51000 Rijeka, Croatia
Phone: +385 (51) 770 447
Fax: +385 (51) 686 166
www.intechopen.com

中国上海市延安西路65号上海国际贵都大饭店办公楼405单元
Phone: +86-21-62489820
Fax: +86-21-62489821

IntechOpen

IntechOpen